

In vivo spectroscopic ellipsometry measurements on human skin

Danny Chan
Benjamin Schulz
Kathrin Gloystein
Heike Hedwig Müller
Michael Rübhausen

Universität Hamburg
Institut für Angewandte Physik
Jungiusstrasse 11
Hamburg 20355, Germany

Abstract. We study the behavior of optical properties of human skin across its layers. We describe ellipsometric measurements for spectrally resolved *in vivo* investigations of biological tissue. We show *in vivo* measurements on human skin of the ellipsometric parameters Ψ and Δ , which describe the change in polarization of light on reflection on a sample. A tape-stripping study reveals the depth profile of the ellipsometric parameters into the stratum corneum. The depth profile shows an increase in both quantities with increased depth. Analyzing the development of Ψ on the number of strips using an exponential function shows a steady state after approximately 2 μm . The evolution of Ψ and Δ can be described using a morphological model containing an effective medium approximation accounting for the water content of the skin, surface roughnesses of the corneocytes, as well as the alternating cell and lipid layers. © 2007 Society of Photo-Optical Instrumentation Engineers. [DOI: 10.1117/1.2435703]

Keywords: ellipsometry; tissues; spectroscopy; anisotropy; matrix multiplication.

Paper 06056R received Mar. 9, 2006; revised manuscript received Sep. 18, 2006; accepted for publication Nov. 15, 2006; published online Feb. 8, 2007.

1 Introduction

Skin is usually described as consisting of two major layers, the dermis and the epidermis. The main dermis constituents are collagen, elastic tissue, and blood vessels, and it acts as a supportive layer for the epidermis.¹ The main epidermis function is maintenance, yielding a continuous renewal of the skin's outermost layer, the stratum corneum.

In the epidermis, keratinocytes move from the basal cell layer up to the stratum corneum and undergo dramatic structural as well as biochemical changes. In the stratum corneum, the keratinocytes become dead cornified cells, so called corneocytes, which shed off the skin by the daily mechanical and chemical wear. They are replaced by the on-moving keratinocytes from below. The stratum corneum functions as a highly efficient barrier for the body against chemical and biological agents. It facilitates prevention of dehydration of the organism and protection. This is possible by the combination of highly packed keratin filaments in the cells and lipid layers surrounding the cells, resulting in a barrier that is impermeable for hydrophobic agents. While highly efficient, the stratum corneum has only a thickness of 10 to 100 μm , depending on the position on the body and its exposition to mechanical wear.

The optical properties of skin are still subject to discussion.² Since the optical parameters are dependent on the structural and chemical properties of the material, it is clear that the rapid biochemical change of the keratinocytes across the epidermis as well as the difference in water content from physiological levels to environmental levels will result in a

change in refractive index and absorption coefficient of the material.

The refractive index of tissues is sometimes estimated using the known dispersion of its main constituents, or measured using destructive methods.^{2,3} The refractive index is then assumed to be the same over the whole depth of the skin, and the layered structure of the skin is not taken into account. Other approaches to measure optical parameters of tissues are, e.g., optical coherence tomography and depolarization measurements. They can help only in acquiring⁴⁻⁶ depth profiles for the refractive index n . The absorption coefficient k cannot be acquired with these techniques. However, the absorption coefficient k is a quantity necessary to completely describe optics in tissues. Therefore, a technique that is able to measure both parameters is required. Ellipsometry can measure these two quantities within one single measurement. Therefore, the complete complex refractive index containing as the real part the refractive index n and as the imaginary part the absorption coefficient k can be measured. Furthermore, ellipsometry does not rely on depolarization of light on scattering in all directions, but uses only the directly reflected light to determine the complex refractive index. Knowledge of the behavior of the complex refractive index over the skin can deliver data about the changes that occur during the differentiation of the keratinocytes. Also, knowledge of the depth-dependent complex refractive index of skin is important for the interpretation of other optical techniques. Scattering methods usually profit greatly from a detailed knowledge of the refractive index, since this is required to estimate the optical path length.³ Determining information for numerous structural parameters of the skin out of one single, fast measurement is

Address all correspondence to Benjamin Schulz, Institute of Applied Physics, University of Hamburg, Jungiusstrasse 11, Hamburg 20355, Germany; Tel: 49 40 42838-2341; Fax: 49 40 42838-4368; E-mail: ben99@gmx.net

highly desirable and can be achieved using spectrally resolved ellipsometry.

In this paper, we propose to use the advantages of spectral ellipsometry such as low power density, high sensitivity, and gathering many parameters within one single and fast measurement on *in vivo* tissue. Our study found that the optical ellipsometry technique is highly sensitive to both the biochemical and the morphological parameters of skin. The feasibility of *in vivo* measurements is demonstrated with a tape-stripping method, in which we study the variation of the ellipsometric parameters Ψ and Δ as a function of depth into the stratum corneum. The tape-stripping procedure changes the morphology of the skin in a relatively controlled way. The variation of the ellipsometric parameters can be described by the change in complex refractive index across the stratum corneum and by assuming a model accounting for interface roughnesses and the alternating corneocyte and lipid layers. The model yields structural parameters such as corneocyte thicknesses, lipid layer thicknesses, and surface roughness parameters, which are within a sensible region. Once a model has been established, all of these parameters can be determined from single measurement.

2 Experimental Details

2.1 Ellipsometry

Ellipsometry is a technique for establishing optical and structural parameters of complex layered systems. It is known in solid state physics for its accuracy and the low power densities in the probe beam that hardly influence the samples.⁷

In ellipsometry, linear or circular polarized light is reflected by the sample under an angle ϕ_0 . The change in polarization on reflection is analyzed using a rotating polarizer.

The measured intensity changes are converted to the ellipsometric parameters Ψ and Δ , which are linearly independent. These parameters signify the change in polarization due to the refractive index mismatch between different structural features of the system and are restricted to the range 0 to 360 deg. They are calculated using only intensity ratios measured at different analyzer angles. Therefore, this technique is self-normalizing, which results in its high accuracy. The basic equation for ellipsometry is

$$\rho = \tan(\Psi)e^{i\Delta} = \frac{R_p}{R_s}, \quad (1)$$

where R_p and R_s are the complex reflection coefficients for the components of the light being parallel and perpendicular to the plane of incidence, respectively⁷ (see Fig. 1).

The ellipsometer used for all measurements is a Sentech SE850 with custom-made extensions for the deep-UV region. Its light source in the visible and UV wavelength range is a xenon gas discharge lamp. The light is coupled into the arm emitting the light via a glass fiber. The reflected light is coupled into a second glass fiber and detected using a grating and a photodiode array. The usage of a photodiode array enables the detection of the whole wavelength region from 220 to 790 nm in one measurement. To compensate for the high surface roughness of the skin, focusing units were used for all measurements. These microprobes focus the emergent beam from a diameter of 6 mm down to a diameter of 200 μm .

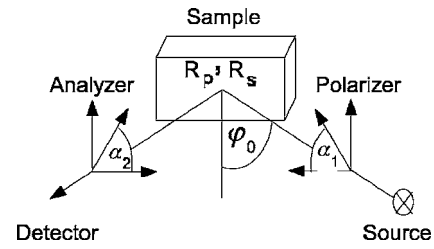


Fig. 1 Basic layout of an ellipsometry measurement. Light is emitted by the source S and linearly polarized with a polarizer angle α_1 . The intensity of the directly reflected light under an angle ϕ_0 is measured at the detector D as a function of the analyzer angle α_2 .

Since Eq. (1) assumes a parallel beam, it must be integrated over the angles given by the usage of a focused beam. Test measurements on silicon wafers, however, show that the resulting error can be estimated to be less than 10^{-2} in n and k for our lenses with a small numerical aperture and, therefore, weak focusing.

2.2 Basic Equations

The ellipsometric parameters Ψ and Δ describe the change in polarization of the light beam due to the influence of a sample. To extract the physical parameters of the sample like refractive index, one must make a model of the investigated system.

Assuming a homogeneous, infinitely thick sample, or a so-called bulk system, the reflection parameters R_p and R_s from Eq. (1) are the well-known Fresnel coefficients, and the ellipsometric parameters can be transformed into the complex refractive index of the sample N_1 according to

$$N_1 = N_0 \tan \phi_0 \left[1 - \frac{4\rho}{(1+\rho)^2} \sin^2 \phi_0 \right]^{1/2}, \quad (2)$$

where N_0 is the complex refractive index of the ambient, which is usually air and can be set in good approximation to 1. In this case, the values of Δ are restricted⁷ to 0 to 180 deg.

To model the influence of small particles with refractive index N_b embedded in a host medium with refractive index N_h , the effective medium approximation is used. It states that the net effect of both constituents can be modeled as a single medium with complex refractive index N_e given by

$$\frac{N_e^2 - N_h^2}{N_e^2 + 2N_h^2} = f_b \frac{N_b^2 - N_h^2}{N_b^2 + 2N_h^2}, \quad (3)$$

where f_b is the volume percentage of the embedded material.⁷

A sample consisting of homogeneous, isotropic layers where each layer is characterized by its complex refractive index can be modeled using a matrix formalism.⁷ The different layers are modeled by 2×2 matrices. For each polarization component, the interface between two layers A and B is described by an interface matrix \mathbf{I}_{AB} , which accounts for the change in polarization due to index mismatch between the layers and depends on the Fresnel coefficients of the interface. The change in polarization due to the thickness and the complex refractive index of a layer A is modeled by a layer matrix \mathbf{L}_A . From the matrix product of the interface and layer matri-

ces of all layers 2×2 scattering matrices \mathbf{S}_p and \mathbf{S}_s for both linear polarization components can be computed

$$\mathbf{S}_{s,p} = \mathbf{L}_{01s,p} \mathbf{L}_1 \mathbf{L}_{12s,p} \mathbf{L}_2 \cdots \mathbf{L}_n \mathbf{L}_{n(n+1)s,p}. \quad (4)$$

Here, the indexes p and s refer to the parallel and the perpendicular polarizations.

The ratio of the complex reflection coefficients R_p/R_s required to analyze Eq. (1) can then be calculated to be

$$\frac{R_p}{R_s} = \frac{\mathbf{S}_{21p}}{\mathbf{S}_{11p}} \cdot \frac{\mathbf{S}_{11s}}{\mathbf{S}_{21s}}. \quad (5)$$

The influence of surface roughnesses, which are much smaller than the incident wavelength, can be modeled in this framework by introducing a roughness layer. The complex refractive index of the roughness layer is then given by an effective medium approximation where the two constituents are given by the two adjacent layers.⁷

Equation (5) cannot be analytically inverted for the unknown parameters. Therefore, it must be fitted numerically to the measured spectra to yield the parameters of interest, such as complex refractive indices, layer thicknesses, inclusion ratios in layers described by effective medium approximations, and roughness parameters.

2.3 Experiment

The skin of the left middle finger just above the nail from different volunteers was measured by *in vivo* ellipsometry. No special treatment was performed prior to the measurements. To immobilize the arm we used a custom made arm rest. Measurements were performed in a wavelength range from 300 to 780 nm. Layers of skin were removed with a tape stripping procedure. Adhesive tape was applied onto the skin and ripped off. With each strip, approximately one cell layer is removed with a thickness of about 200–500 nm. This procedure should be effective up to about 10 strips, since after that the glue does not stick to the corneocytes effectively.⁸ After a tape strip, ellipsometric measurements were performed. For the measurement, the sample was moved through the focus and the raw intensity spectrum at defined polarizer and analyzer angle was observed. The measurement was started when the raw intensity reached its maximum value. The acquisition time for one spectrum was 20 seconds.

Since the immobilization of the hand was not perfectly achieved, at least five measurements were made for each strip. The maximum intensity, which should stay roughly constant during one measurement, was monitored online. Loss of the focus position due to movements of the hand was thereby identified, and the corresponding measurements were not considered in the analysis. Up to 55 strips were performed.

To reduce the effects due to the hand moving between the measurements, the spectra belonging to the same strip were averaged. Furthermore, mean values of several wavelength regions of the averaged spectra were computed, because the spectral features of the measurements can vary considerably between measurements due to the local variations in morphology and chemical composition of the skin resulting from slightly different positions of the beam. Also, movements during a single measurement can alter the spectral information.

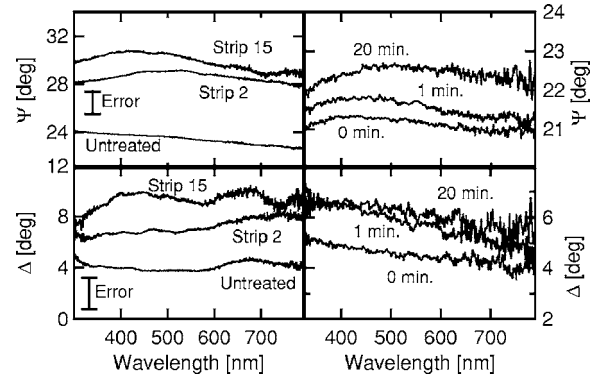


Fig. 2 Left column, averaged Ψ and Δ spectra for different tape strips from one person; right column: Ψ and Δ spectra of human fingernails after different immersion times in water.

3 Results

Figure 2 shows averaged spectra of Ψ and Δ from different tape strips of one person and a comparison to previous hydration experiments on human fingernails.⁹ The error bar signifies the standard deviation of five measurements. It can be seen that with increasing strip number both Ψ and Δ are increasing. The change in both parameters is larger than the error bars, resulting from averaging the measurements belonging to one strip. The changes in Δ are less distinct, which is not surprising, since the determination of Δ in ellipsometry is more difficult for nearly transparent media such as the stratum corneum.

The observed behavior of Ψ and Δ is similar to the results of previous hydration experiments *in vitro* on human fingernails.⁹ The increase in Ψ can be explained by an effective medium taking into account the skin host medium and water. The increase in Δ cannot be understood in this model. For transparent media such as water, the value of Δ approaches zero. Therefore, an increase in water content alone would result in an decrease of Δ . The increase can be understood, however, by taking into account the presence of water bound by hydrogen bonds to the protein matrix.⁹ Also, other chromophores such as melanin, which introduce additional absorptions, become more important with increased depth into the skin.¹⁰ Finally, a layered structure of the sample can influence the behavior of the ellipsometric parameters as well.

The wavelength averaged Ψ spectra were plotted against the strip number and fitted with an exponential function

$$\Psi(x) = K_0 + K_1 \exp(-K_2 x). \quad (6)$$

Figure 3 shows the result of this fit for a wavelength average from 400 to 500 nm for three different persons. The values for the parameters in Eq. (6) can be found in Table 1. Initial values of Ψ are around 24.5 with a decay constant $t = 1/K_2$ of 1 to 4. With a steady state criterion of $1/e$, we can see that after approximately $2 \mu\text{m}$ a steady state is reached, assuming that each layer has a thickness of $0.5 \mu\text{m}$. This is in accord with previous publications,⁸ which showed that the adhesive tape loses its effectiveness in removing cells after a few strips. Only for at most the first 10 tape strips one can therefore expect that a tape strip removes a single cell layer.

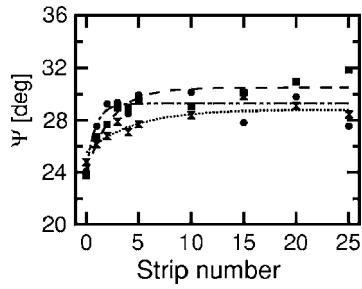


Fig. 3 Mean value of averaged Ψ spectra in the wavelength region 400 to 500 nm versus tape strip number from three different volunteers; lines are fits of Eq. (6) to the measurements.

The differences between the development of Ψ of different persons can be attributed to the interindividual biological variations.

3.1 Modeling

While a qualitative explanation of the development of Ψ and Δ can be made as already outlined, a simple bulk model according to Eq. (2) is not sufficient to describe the spectra. A conversion using the simple bulk model from Eq. (2) results in spectra that have values of $n \approx 1.33$.

Since the refractive index of water is $n \approx 1.33$ in the visible,¹¹ a higher water content in the skin layer results in a lowering of the observed n toward 1.33, because water is the dominant constituent of biological media. A decrease below this value is unlikely, since the other constituents of skin can be expected to be optically denser. Thus, n should always be larger than 1.33.

A first analysis applying an effective medium approximation using Eq. (3) with tissue host material and embedded water droplets was only able to describe the spectra of Ψ , but not the spectra of Δ . Taking into account that the refractive index n is mostly influenced by Ψ , and that the absorption coefficient k is mostly influenced by Δ , this result can be seen as clear evidence not only for applying a more realistic model, but also that it is necessary to have information about the absorption coefficient k to completely understand the optical parameters in tissues. A better description of the spectra of both Ψ and Δ can be achieved only by assuming a model that accounts for surface roughness effects and the internal structure of the stratum corneum. The model is schematically depicted in Fig. 4. It assumes four constituents, a dry host medium, a medium comprised of skin lipids, water, and air. Using Eqs. (4) and (5), the alternating occurrence of corneocytes and lipid layers is modeled by an alternating sequence

Table 1 Values of the fit parameters for Eq. (6) of the measurements shown in Fig. 3.

	K_0	K_1	K_2
Squares	30.47	-6.6	0.43
Circles	29.25	-5.19	1.18
Triangles	28.79	-3.28	0.23

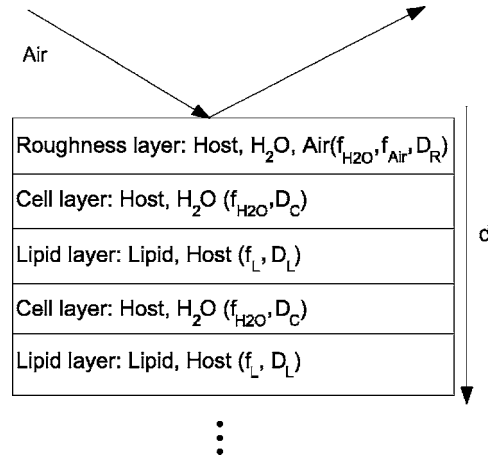


Fig. 4 Morphological model of the stratum corneum with surface roughness (f_{Air} , air content; D_R , roughness layer thickness) and alternating cell and lipid layers (f_{H_2O} , water content; D_C , cell layer thickness; D_L , lipid layer thickness; f_L , lipid content; and d , distance into the skin).

of isotropic, homogeneous layers. An effective medium of the host material and water with a volume ratio of f_{H_2O} constitutes the cell layer material. Another effective medium of the same host material and the skin lipids with volume ratio f_L constitutes the lipid layer material. The thicknesses of the cell and lipid layers are given by the parameters D_C and D_L , respectively. Finally, the roughness is modelled by an effective medium of the cell layer and air with volume ratio f_{Air} and a layer thickness D_R . Up to six subsequent corneocyte and lipid layers were used in the modeling. The analysis of a representative measurement is described in the following.

For this analysis, the water content f_{H_2O} was assumed to follow a gradient, as given in Fig. 5 with values ranging from 15 to 19%. For this gradient, it was assumed that the development of the water content follows the same behavior as the measured values of Ψ , as shown in Fig. 3. To determine the refractive indices and absorption coefficients of the host medium and the lipid layer, the four parameters were assumed to be constant over the whole wavelength range. The assumption of a constant host dispersion is reasonable, as previous measurements on nails as a biochemically similar system showed a mostly flat dispersion.⁹ Then a simultaneous fit of the first five tape strips was made, where the refractive indices and the absorption coefficients of host and lipid layer were equal for each strip. This fit results in estimates for the unknown optical constants of the host and the lipid medium.

The complex refractive indices derived in the first step were then used in fits of every single tape strip measurement. Therefore, only the roughness parameters, the layer thicknesses, and the inclusion percentage in the lipid layer were varying parameters in the optimization procedure.

The result of a such a fit to the measured ellipsometric parameters is shown in Fig. 6. It can be seen that the modeling of surface roughnesses and the internal structure results in an additional oscillation that effectively offsets the resulting Ψ to a higher value. Also, the shape of the spectrum is qualitatively followed by the fitted data.

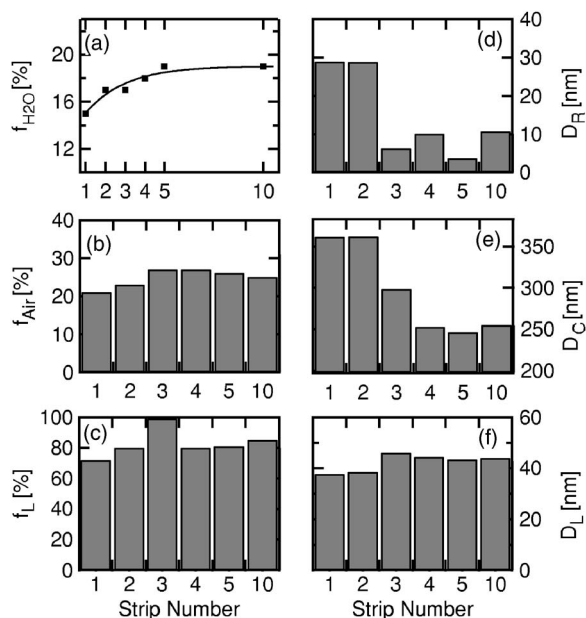


Fig. 5 Fit results for the measurements on one person: (a) assumed water content development f_{H_2O} , (b) air content f_{Air} of the roughness layer, (c) lipid content f_L of the lipid layer, (d) thickness D_R of the roughness layer, (e) thickness D_C of the cell layer, and (f) thickness D_L of the lipid layer.

The numerically fitted values of the layer thicknesses and the effective media inclusions are given in Fig. 5. The thickness of the roughness layer D_R drops sharply from values of approximately 30 to values below 10 nm, while the air content stays roughly constant at around 27%. This is consistent with the view that for the first strips, the surface roughness of a corneocyte is dominated by the surface proteins, e.g., desmosomes with typical dimensions of up to 50 nm. For subsequent strips, the surface roughness of the cell is diminished, since the break occurs within the lamellar lipid layer. At the same time, the thickness of the corneocytes D_C shows values

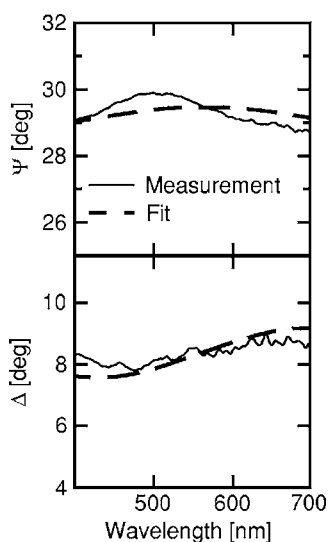


Fig. 6 Representative fit for tape strip 5: full line, measurement data; dashed line, fit result.

Table 2 Values of the optical parameters assuming a constant dispersion for the cell layer composed of the host material and water.

Tape Strip	Refractive Index n	Absorption Coefficient k
1	1.421	0.231
2	1.420	0.228
3	1.419	0.225
4	1.418	0.223
5	1.417	0.220
10	1.417	0.220

The host material has values of $n=1.436$ for the refractive index and $k=0.273$ for the absorption coefficient. The lipid layer has values of $n=1.471$ and $k=0.273$. The values for the lipid layer are independent from the depth in the stratum corneum, and therefore from the tape strip number.

of around 350 to 250 nm. This is within the expected range, since a single corneocyte has a thickness¹² of 200 to 500 nm. Finally, the percentage of lipids in the lipid layer has a high value of 80% and more, while the thickness of the lipid layer has a value of approximately 40 to 45 nm. Again, this is consistent¹³ with values for the thickness of the lipid lamella of 40 to 60 nm.

The values for the parameters of the complex refractive index, the refractive index n , and the absorption coefficient k of the cell layers of the strips, thereby the depth profile of these parameters, are given in Table 2. The host material has values of $n=1.436$ for the refractive index and $k=0.273$ for the absorption coefficient. The lipid layer has values of $n=1.471$ and $k=0.273$. The values for the lipid layer are independent from the depth in the stratum corneum, and therefore from the tape strip number.

4 Conclusion

The measurements and the mathematical analysis performed in this paper demonstrate that ellipsometry can be used to investigate tissues *in vivo*.

The low power density is advantageous for *in vivo* measurements. In particular, we performed an *in vivo* tape strip study of human skin. The tape-stripping removes subsequent cell layers of the skin, resulting in a scan through the various depths of the stratum corneum.

The behavior of the ellipsometric parameters Ψ and Δ can be modeled using a model with interface roughnesses and alternating corneocyte and lipid layers. Assuming a water content from 15 to 19%, we derive values for the roughness parameters of $D_R=30$ nm and $f_{Air}\approx 27\%$. The calculated values for the corneocyte thickness of $D_C=350$ to 250 nm and the parameters for the lipid layers of $D_L=40$ to 45 nm and $f_L\approx 80\%$ are within the range of published values.

Once the model has been established, we can determine a number of parameters for which one would usually require more than one measurement. This is of great importance when studying the “functional behavior” in bioorganic tissues, as you can study many parameters simultaneously.

The further development of the experimental instrumentation, the extension of our model to other important chromophores of the skin, and the further understanding of the important morphological parameters are the focus of our work.

More studies applying the spectral ellipsometry to bioorganic tissue *in vivo* and *ex vivo* are being completed.

Acknowledgments

We thank M. Berneburg and R. Wepf for many discussions. We acknowledge financial support for this work via Beiersdorf AG Hamburg and DFG through Ru 773/2-2 and Ru 773/2-3.

References

1. F. Parker, *Structure and Function of the Skin*, pp. 1–14, Prentice Hall International, London (1991).
2. F. P. Bolin, L. E. Preuss, R. C. Taylor, and R. J. Ference, "Refractive index of some mammalian tissues using a fiber optic cladding method," *Appl. Opt.* **28**, 2297–2303 (1989).
3. T. L. Troy and S. N. Thennadil, "Optical properties of human skin in the near infrared wavelength range of 1000 to 2200 nm," *J. Biomed. Opt.* **6**, 167–176 (2001).
4. A. Knüttel, S. Bonev, and W. Knaak, "New method for evaluation of *in vivo* scattering and refractive index properties obtained with optical coherence tomography," *J. Biomed. Opt.* **9**, 265–273 (2004).
5. S. L. Jacques, J. C. Ramella-Roman, and K. Lee, "Imaging skin pathology with polarized light," *J. Biomed. Opt.* **7**(3), 329–340 (2002).
6. A. G. Matoltsy and C. A. Balsamo, "A study of components of the cornified epithelium of human skin," *J. Biophys. Biochem. Cytol.* **1**(4), 339–360 (1955).
7. R. M. A. Azzam and N. M. Bashara, *Ellipsometry and Polarized Light*, 4th ed., Elsevier Science B.V., Amsterdam (1999).
8. F. Pflücker, H. Hohenberg, E. Hölzle, T. Will, S. Pfeiffer, R. Wepf, W. Diembeck, H. Wenck, and H. Gers-Barlag, "The outermost stratum corneum layer is an effective barrier against dermal uptake of topically applied micronized titanium dioxide," *Int. J. Cosmet. Sci.* **21**, 399–411 (1999).
9. B. Schulz, D. Chan, J. Bäckström, M. Rübhausen, K. P. Wittern, S. Wessel, R. Wepf, and S. Williams, "Hydration dynamics of human fingernails: an ellipsometric study," *Phys. Rev. E* **65**, 061913-1–061913-7 (2002).
10. A. R. Young, "Chromophores in human skin," *Phys. Med. Biol.* **42**, 789–802 (1997).
11. J. D. Jackson, *Classical Electrodynamics*, Wiley, New York (1975).
12. T. Richter, J. H. Müller, U. D. Schwarz, R. Wepf, and R. Wiesendanger, "Investigation of the swelling of human skin cells in liquid media by tapping mode scanning force microscopy," *Appl. Phys. A* **72**(Suppl.), 125–128 (2001).
13. G. H. Imokawa, H. Kuno, and M. Kawai, "Stratum corneum lipids serve as a bound-water modulator," *J. Invest. Dermatol.* **96**, 845–851 (1991).